Modeling and Analysis of a Micro-Grid System Powered by Renewable Energy Sources

R. Ahshan[*], M.T. Iqbal, George K. I. Mann and John E. Quaicoe

Faculty of Engineering and Applied Science, Memorial University of Newfoundland, St. John's, NL, Canada A1B 3X5

Abstract: Renewable source based micro-generations such as wind and hydro offer the best potential for emission free power in future power systems. This paper investigates the technical issues related to stable and autonomous operation of a micro-grid system consisting of renewable power sources. A small hydro generation unit and a wind farm are the main renewable power generation units in the proposed micro-grid system. The system under investigation represents a case study in Newfoundland and Labrador, Canada. The availability of the utility grid and the intermittent nature of wind power generation are taken into consideration when identifying the operational modes of the proposed micro-grid system. The investigations are carried out through dynamic modeling and simulation of the proposed micro-grid system in different operational modes. The components models of the proposed micro-grid system are also presented in this paper. The investigations reveal that appropriate control techniques are required to be developed depending upon the operational modes of the proposed system with some additional arrangements. Such arrangements include the type of energy storage unit, reactive power compensation, the management of excess power in the system due to the wind generator etc. The control concepts with additional necessities are also outlined in this paper. This paper concludes that the development of such control concepts is essential to ensure stable and automatic operation of the proposed micro-grid system while maintaining the system voltage and frequency in their rated values.

Keywords: Renewable energy, distributed generation, micro-grid, system, modeling and simulation.

INTRODUCTION

The demand for more power combined with interest in clean technologies has driven researchers to develop distributed power generation systems using renewable energy sources [1]. However, the integration of a large number of distributed generations into distribution networks is restricted due to the capacity limitation of the distribution networks and their unidirectional power flow behaviours [2]. Such barriers have motivated researchers to find alternative solutions to enhance the integration of distributed generation into the distribution networks. An alternative approach called "Micro-grid" was proposed in 2001 as a means of integrating distributed generations into the distribution networks [3].

Micro-grid (MG) is the combination of loads, micro-generation (or distributed generation) units, storage systems, and associated power conditioning units that operates as a single controllable system and provides power or both power and heat to loads. Distributed generation in micro-grid operation can provide benefits to the utility operators, distributed generation owners and consumers in terms of reliable power supply, efficient power transmission, reduction in transmission system expansion, and enhancement of renewable power penetration.

A review of the existing literature reveals that the first micro-grid architecture is called the Consortium for Electric Reliability Technology Solutions or CERTS micro-grid [3]. The CERTS micro-grid system is the combination of inverter-interfaced distributed generation (DG) units. Such DG units can be based on both renewable and non-renewable energy sources. Each DG unit has its own battery-based storage system connected to the DC-link of the inverter. The control system for each inverter-interfaced DG unit is developed and tested with a laboratory prototype.

Barnes *et al.* also proposed a micro-grid system under the frame of the European project "Micro-grid". Such micro-grid architecture consists of two photovoltaic (PV) generators, one wind turbine (WT), battery storage, controllable loads and a controlled interconnection for the local low voltage grid. The battery inverter system in this micro-grid is employed to control the system voltage and frequency during isolated operation [4]. Moreover, a simulation platform is developed to simulate the steady-state and dynamic operation of low voltage three phase networks that include DG units such as WTs, fuel cells (FCs), PV systems and micro-turbines [5, 6].

The New Energy and Industrial Technology Development Organization (NEDO) in Japan proposed three micro-grid projects in 2003. The first NEDO micro-grid (1.7MW) system is comprised of different kinds of fuel cells such as the molten carbonate fuel cell (MCFC), phosphoric acid fuel cell (PAFC), solid oxide fuel cell (SOFC), and PV system and battery storage. A combination of the different kinds of fuel cells as the main energy sources (81 percent of the total

*Address correspondence to this author at the Faculty of Engineering and Applied Science, Memorial university of Newfoundland, St. John's, NL, Canada A1B 3X5; Tel: 1-709-864-3472;
E-mail: rahshan05@gmail.com
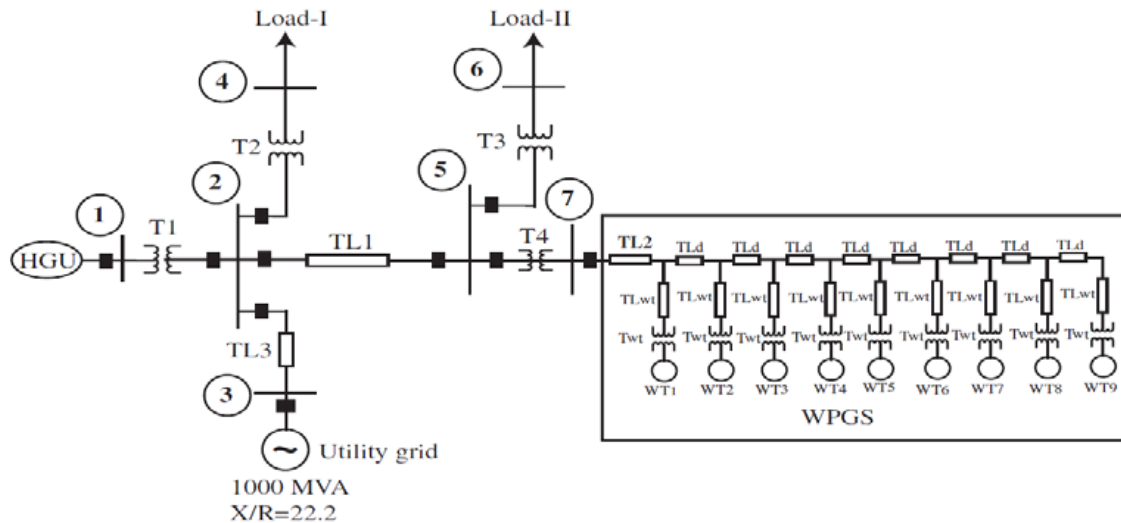
Fig. (1). One-line diagram of the micro-grid system at Fermeuse, Newfoundland and Labrador, Canada.

generation capacity) is the key feature of the first NEDO micro-grid. The second NEDO micro-grid (610kW) configuration consists of PV, WT, biomass and battery storage. The main feature of such a system is the combination of renewable energy sources. The third NEDO micro-grid (750kW) system consists of PV, WT, MCFC, biogas and battery bank, which has a very low percentage (13 percent) of renewable energy generation [6, 7].

Micro-grid research in Canada started in universities with the cooperation of the CANMET energy technology center at Varennes [6]. This research group identified industry cases, such as the isolated Ramea wind-diesel micro-grid system and the Fortis Alberta grid-tied micro-grid system for investigation. The Ramea wind-diesel micro-grid system consists of six 65 kW fixed speed WTs and diesel generators. Additionally, three 100 kW rated WTs are currently being installed to integrate with the existing system. The Fortis-Alberta grid-tied micro-grid system consists of 3 MW run-of-river hydro and 3.78 MW fixed speed wind turbine generation units [8]. Canada's micro-grid research and development has evolved to develop a test bed for industrial-grade prototype testing and performance evaluation [6].

A study of micro-grid dynamic behaviour, along with the control of the micro-generation units is presented by F. Kateraie. This micro-grid system is based on the benchmark system of the IEEE Standard 399-1997, which consists of three generation units comprised of a diesel generator or a gas turbine generator, an electronically interfaced distributed generation and a fixed speed wind power generator [9]. Research on micro-grid systems is also found in the literature, where the generation units and loads are arbitrarily assumed [10-12].

MG systems configuration depends on the size and nature of the micro-generation units in the micro-grid, as well as the site and the availability of the primary energy resources on the site, especially for renewable power sources. In this paper, operational and control issues of a micro-grid system are investigated on an existing real system at Fermeuse, Newfoundland, Canada. It is to be noted that the study system in this research consists of wind and hydro

power generation units to serve power in a micro-grid domain. Dynamic modeling of such a micro-grid system is essential to carry out investigations regarding operation and control of the system. It is seen that most of the inverter-interfaced micro-generation units are represented by an equivalent DC source in the system modeling, which does not account for the dynamics of the micro-generations. Consideration of dynamics of micro-generation units is required for micro-grid system analysis because a change in input mechanical power of a micro-generation unit can affect the micro-grid system operation and control. This is because of low inertia in the micro-grid system as compared to a conventional power system. Therefore, modeling micro-grid systems with the dynamics of micro-generation units can be the better approach for investigating the operation and control issues of a micro-grid system.

This paper presents a dynamic model of a proposed micro-grid system that consists of stochastic renewable power generation sources. This model is able to reflect micro-grid system behaviours during its operational modes. It is worth mentioning that the system behaviours explore the technical challenges regarding operation and control of the proposed micro-grid system. The following sections of this paper are organized to present the proposed micro-grid system description, operational modes of the micro-grid system, components model of the micro-grid system, simulation results discussions and problem identifications, and a brief outline of the proposed control concepts. Finally some conclusions are presented.

THE MICRO-GRID SYSTEM

The one-line diagram of the micro-grid system shown in Fig. (**1**) consists of a Hydro Generation Unit (HGU), a Wind Power Generation System (WPGS), and two load areas represented as Load-I and Load-II. The two load areas are connected through a TL1 km transmission line and the two generating systems are connected through a (TL1+TL2) km transmission line. The WPGS is connected to bus 7 through a TL2 km transmission line and a 12.5/66kV, 45 MVA power transformers. Each turbine in WPGS is separated from each other by TLd km. Load-II is connected to bus 6 and the

Table 1. Bus Data for Fermeuse Micro-Grid System: Buses

BUS	P[MW]	Q[MVAR]	V[kV]
1	7.3	6.8	6.9
2	ΔP_E	ΔQ_E	66
3	ΔP_E	ΔQ_E	66
4	3.94	0.95	12.5
5	0	0	66
6	2.82	0.6	12.5
7	27	12	12.5

Table 2. Bus Data for Fermeuse Micro-Grid System: Transmission Lines and Transformers

Components	V[kV]	Z[Ω]	S[MVA]
TL1	66	0.0416 + j0.0663	50
TL2	12.5	0.0374 + j0.3741	45
TL3	66	0.002 + j0.0032	75
TLd	12.5	0.00072 + j0.0012	45
TLwt	12.5	0.00006 + j0.000096	5
T1	6.9/66	0.0854 + j0.8541	10
T2	66/12.5	0.0493 + j0.493	5
T3	66/12.5	0.061 + j0.62	4
T4	66/12.5	0.05 + j0.5	50
Twt	1/12.5	0.006 + j0.0625	5
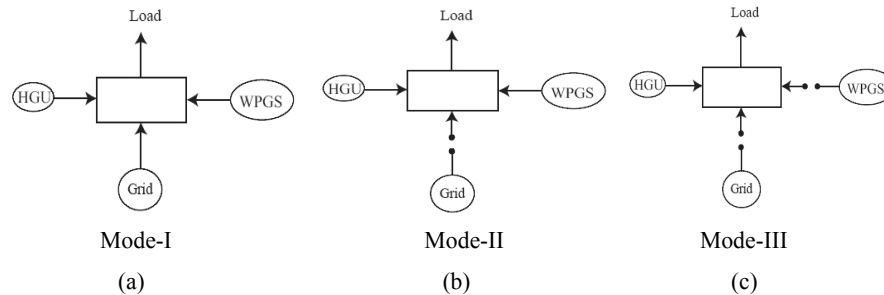
Fig. (2). (**a**). Mode-I: Grid connected system, (**b**) Mode-II: Isolated system with wind power generation, and (**c**) Mode-III: Isolated system without wind power generation.

power is delivered to the load using a 66/12.5kV, 4 MVA power transformer. Load-I is connected to bus 4 and the power is delivered to the load using a 66/12.5kV, 5 MVA power transformer. The HGU is connected to bus 1 using a 6.9/66kV, 8 MVA power transformer. A conventional synchronous generator, equipped with an IEEE standard excitation and governor system, is used for the HGU. A 66kV, 1000 MVA grid is connected to bus 3. Data for the buses of the proposed micro-grid system are provided in Table **1**, where ΔP and ΔQ can be defined as the excess or deficit in active and reactive powers in the micro-grid system.

Also, the data for transmission lines and transformers are provided in Table **2**.

OPERATIONAL MODES OF THE MICRO-GRID SYSTEM

According to the current regulation of the utility company, the unavailability of the utility grid due to faults or regular maintenance first requires disconnecting WPGS from the grid. Moreover, in the event that the grid power is lost due to faults or scheduled maintenance, a blackout would result because operation of the HGU in isolated mode is not the current practice of the utility owner. Even with only HGU in operation, some load shedding may be necessary since the HGU would not be able to meet the total load demand. Hence the consequences of the grid outage are the key drivers which dictate the operational modes of the proposed microgrid system. In order to classify the technical challenges for the proposed micro-grid system under investigation, three operational modes are considered and are conceptually shown in Fig. (**2**).

- Mode-I-Grid Connected System: During this mode of operation the grid is connected to the micro-grid system and the power generated by HGU and WPGS is delivered to the load and the grid. The reactive power required for the doubly-fed induction generator based wind turbines in the WPGS is provided by the grid during this mode.

- Mode-II-Isolated System with Wind Power Generation: During this mode the grid is isolated from the micro-grid system and the system operates with HGU and WPGS. The power generated by both sources is delivered to the load during this operation.

- Mode-III-Isolated System without Wind Power Generation: During this mode the grid is isolated from the system and concurrently the WPGS is also disconnected from the system due to lack of sufficient wind resources.

COMPONENTS MODEL OF THE MICRO-GRID SYSTEM

Two power generations units including transmission lines and transformers are the main components in the micro-grid system which are modeled and presented in the following sub-sections.

WIND POWER GENERATOR

Wind Turbine Rotor

The relation between wind velocity and the rotor output power of a WT is expressed as

$$P_{ro} = 0.5\rho A_{SA} C_p(\lambda, \beta) v_w^3 \tag{1}$$

Tip speed ratio λ is the quotient of linear speed of the tip of the blades to the rotational speed of the WT and is expressed as [13]

$$\lambda = \frac{\omega_m R_t}{v_w} \tag{2}$$

The effects of the different $C_p - \lambda$ curves for various types of wind turbine are negligible, while the electrical behaviour of a system is of interest [13]. Therefore, the analytical approximation of the $C_p - \lambda$ characteristics is considered for rotor modeling as [14]

$$C_p(\lambda, \beta) = 0.5176(\frac{116}{\lambda_i} - 0.4\beta - 0.5)e^{\frac{-21}{\lambda_i}} + 0.0068\lambda \tag{3}$$

and

$$\frac{1}{\lambda_i} = \frac{1}{\lambda + 0.08\beta} - \frac{0.035}{\beta^3 + 1} \tag{4}$$

Doubly-fed Induction Generator

Using *d-q* axis transformation in the synchronously rotating reference frame, the voltages and flux equations for the doubly fed induction generator are written as [15],

$$V_{ds} = r_s i_{ds} - \omega_e \phi_{qs} + \frac{d\phi_{ds}}{dt} \tag{5}$$

$$V_{qs} = r_s i_{qs} + \omega_e \phi_{ds} + \frac{d\phi_{qs}}{dt} \tag{6}$$

$$V'_{dr} = r'_r i'_{dr} - (\omega_e - \omega_r)\phi'_{qr} + \frac{d\phi'_{dr}}{dt} \tag{7}$$

$$V'_{qr} = r'_r i'_{qr} + (\omega_e - \omega_r)\phi'_{dr} + \frac{d\phi'_{qr}}{dt} \tag{8}$$

$$\phi_{ds} = L_{ls} i_{ds} + L_m(i_{ds} + i'_{dr}) \tag{9}$$

$$\phi_{qs} = L_{ls} i_{qs} + L_m(i_{qs} + i'_{qr}) \tag{10}$$

$$\phi'_{dr} = L'_{lr} i'_{dr} + L_m(i_{ds} + i'_{dr}) \tag{11}$$

$$\phi'_{qr} = L'_{lr} i'_{qr} + L_m(i_{qs} + i'_{qr}) \tag{12}$$

The electromagnetic torque is

$$T_{em\_IM} = \left(\frac{3}{2}\right) p(\phi_{ds} i_{qs} - \phi_{qs} i_{ds}) \tag{13}$$

The equation of motion of the rotor is

$$\frac{d\omega_{rm\_IM}}{dt} = \frac{1}{J_{WG}}(T_{em\_IM} - T_{m\_WT} - F\omega_{rm\_IM}) \tag{14}$$

HYDRO POWER GENERATOR

Synchronous Generator

Using *d-q* axis transformation in the rotor reference frame, the voltages and flux equations for the synchronous generator are written as [15],

$$V_d = r_{ss} i_d - \omega_r \phi_q + \frac{d\phi_d}{dt} \tag{15}$$

$$V_q = r_{ss} i_q + \omega_r \phi_d + \frac{d\phi_q}{dt} \tag{16}$$

$$V'_{fd} = r'_{fd} i'_{fd} + \frac{d\phi'_{fd}}{dt} \tag{17}$$

$$V'_{kd} = r'_{kd} i'_{kd} + \frac{d\phi'_{kd}}{dt} \tag{18}$$

$$V'_{kq1} = r'_{kq1} i'_{kq1} + \frac{d\phi'_{kq1}}{dt} \tag{19}$$

$$V'_{kq2} = r'_{kq2} i'_{kq2} + \frac{d\phi'_{kq2}}{dt} \tag{20}$$

$$\phi_d = L_d i_d + L_{md}(i'_{fd} + i'_{kd}) \tag{21}$$

$$\phi_q = L_q i_q + L_{mq}(i'_{kq1} + i'_{kq2}) \tag{22}$$

$$\phi'_{fd} = L_{md} i_d + L_{md} i'_{kd} + (L'_{lfd} + L_{md})i'_{fd} \tag{23}$$

$$\phi'_{kd} = L_{md} i_d + L_{md} i'_{fd} + (L'_{lkd} + L_{md})i'_{kd} \tag{24}$$

$$\phi'_{kq1} = L_{mq} i_q + L_{mq} i'_{kq2} + (L'_{lkq1} + L_{md})i'_{kq1} \tag{25}$$

$$\phi'_{kq2} = L_{mq} i_q + L_{mq} i'_{kq1} + (L'_{lkq2} + L_{md})i'_{kq2} \tag{26}$$

The electromagnetic torque produced by the synchronous machine is

$$T_{em\_SM} = \left(\frac{3}{2}\right) p_{sm}(\phi_d i_q - \phi_q i_d) \tag{27}$$

The equation of motion of the rotor is

$$\frac{d\omega_{rm\_SM}}{dt} = \frac{1}{J_{SM}}(T_{m\_SM} - T_{em\_SM} - F\omega_{rm\_SM}) \tag{28}$$
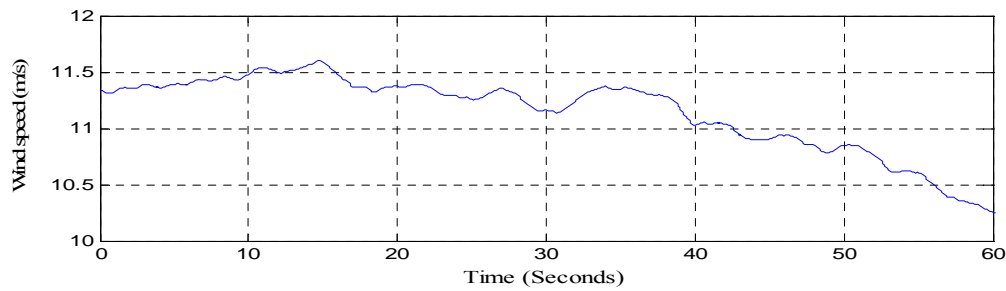
Fig. (3). Wind speed profile used in simulation

Hydro Turbine

The mathematical representation of a single penstock is as follows [16]

$$\frac{dq}{dt} = \left(H_0 - H - H_L\right)\frac{gA_{pen}}{L} \tag{29}$$

where

$$q = G\sqrt{H} \tag{30}$$

Assume that the base flow and base head for rated power output are q_{base} and H_{base} respectively. The per unit representation of (29) is

$$\frac{d\bar{q}}{dt} = \left(1 - \bar{H} - \bar{H}_L\right)\frac{gA_{pen}H_{base}}{Lq_{base}} \tag{31}$$

$$\frac{d\bar{q}}{dt} = \frac{\left(1 - \bar{H} - \bar{H}_L\right)}{T_w} \tag{32}$$

where the water time constant T_W is expressed as

$$T_w = \frac{Lq_{base}}{gA_{pen}H_{base}} \tag{33}$$

The relation between turbine output power and water flow is expressed as follows [16].

$$\bar{P}_m = A_{TG}\bar{H}(\bar{q}_{fl} - \bar{q}_{nl}) \tag{34}$$

Turbine gain A_{TG} is expressed as follows and is used to convert power obtained from the actual gate position to the effective gate position.

$$A_{TG} = \frac{1}{g_2 - g_1} \tag{35}$$

The speed deviation damping due to gate opening is represented by a supplementary term $GD\Delta\omega$, which is subtracted from the output of the turbine model [16].

OTHER COMPONENTS MODEL

Other components such as line, transformer and load are also modeled. The transmission lines are represented by series connected *RL* branches in each phases, given that they are less than 50km in length. A constant impedance load model and a three phase transformer model are used from built in Simulink blocks.

SYSTEM SIMULATION AND SIMULATION RESULTS

The HGU model is a combination of the model of the synchronous generator, hydro turbine and turbine governor system and excitation system. The synchronous machine electrical system is represented by the dynamic equivalent *(d − q)* circuit in a rotor reference frame with the dynamics of stator, rotor and damper windings. The synchronous machine data are obtained from Newfoundland Power, Canada. Synchronous machine rotor and stator parameters can be obtained from [17] and calculated the equivalent parameters for the proposed system. The hydro turbine and turbine governor system model is given in [16]. The parameters for the hydro turbine and penstock are obtained from Newfoundland Power, Canada. The Woodward analog PID governor system is used for the speed control of the synchronous machine. A DC exciter contains the voltage regulator and the exciter is modeled as the excitation system.

The WPGS model consists of the dynamic model of nine variable-speed doubly-fed induction generator based wind turbines. The wind turbine rotor is modeled in terms of the turbine output power, which is the function of the turbine performance co-efficient, air density, and the turbine swept area and wind velocity. The turbine performance co-efficient is also a function of the blade tip speed ratio and the variable blade pitch angle. Vestas-90 wind turbine parameters are used in the developed wind turbine rotor model [18]. A wound rotor asynchronous generator, which allows variable speed operation, is modeled in this research. The rotor winding is connected to the grid using a back-to-back voltage source converter, while the stator is directly connected to the grid. The induction machine electrical system is represented by the dynamic equivalent (d-q) circuit in a synchronously rotating reference frame [15]. Induction generator parameters can be obtained from [19].

The utility grid is represented by an equivalent model of a 66 kV three phase voltage source with the short-circuit capacity of 1000 MVA and reactance to resistance ratio of 22.2 [9]. The parameter information about the line, transformer and load are obtained from the utility company, Newfoundland Power.

Simulations for three operational modes shown in Fig. (**2**) are performed and the simulation results are presented in the following sub-sections. The measurements presented in the simulation results are per unit with a base power of 27 MVA. The simulation was performed for a 60 second interval. In the grid connected mode, all of the nine wind turbines are in operation under wind conditions, whereas in the isolated mode with wind conditions, only one wind turbine is in operation. WPGS with no output power represents the lack of sufficient wind velocity to generate electric power. The wind speed profile in Fig. (**3**), which is the input to the wind turbine rotor, is generated using the wind field model.

(a)

(b)

(c)

(d)

(e)

(f)
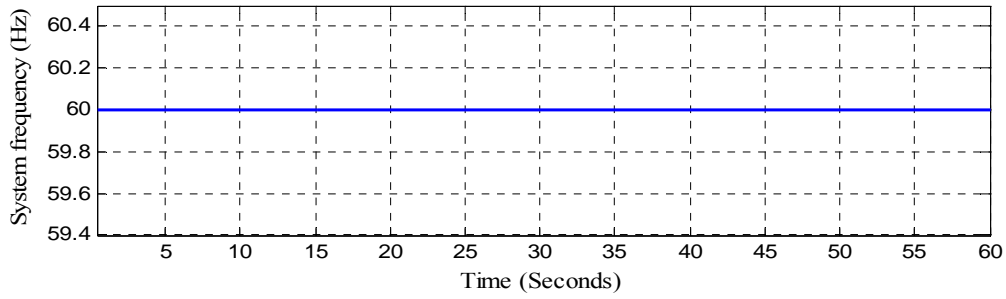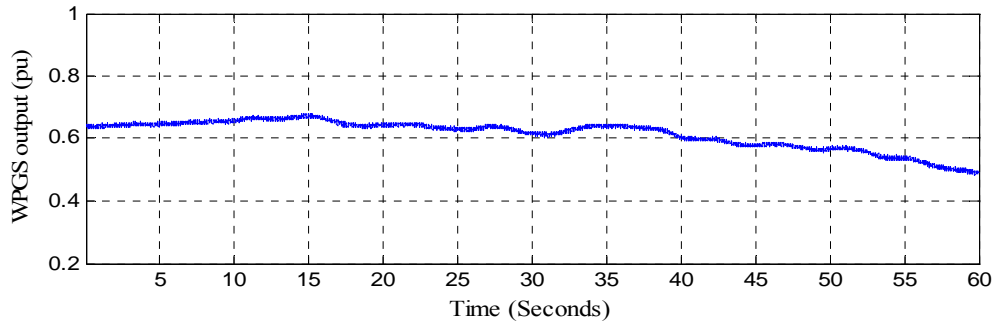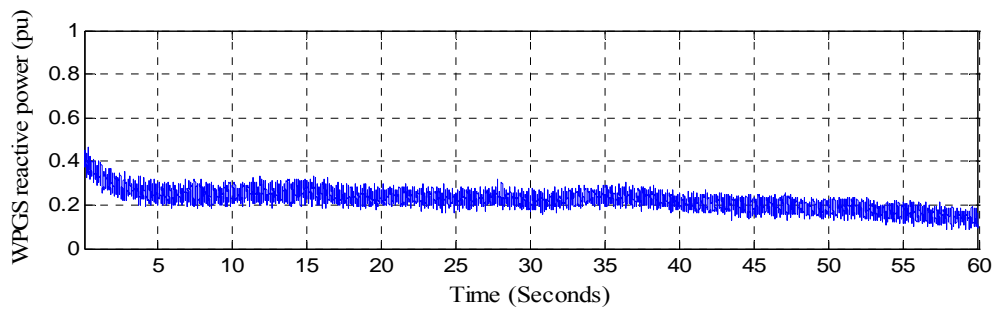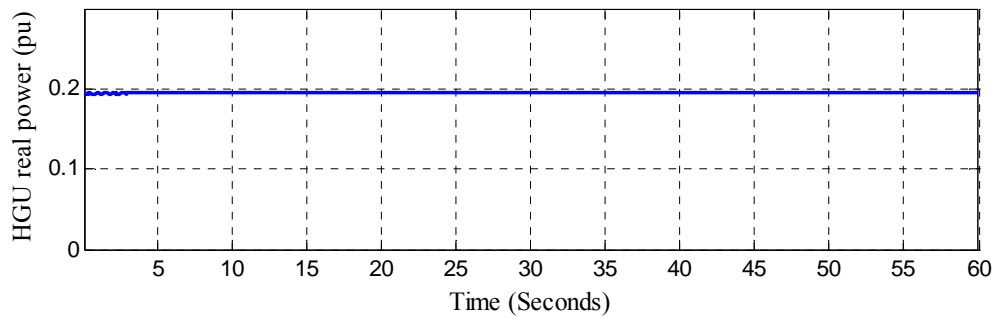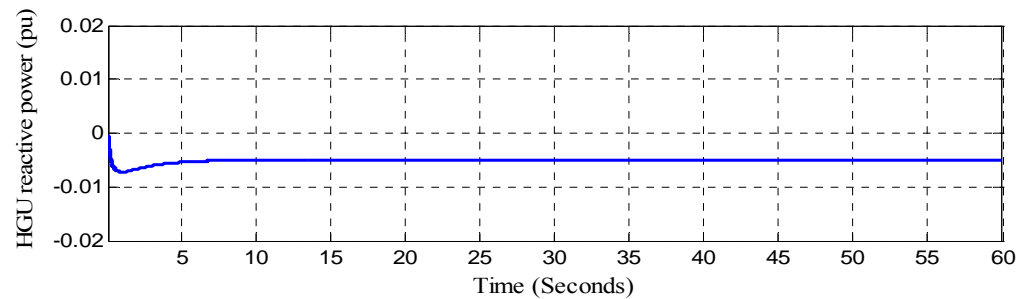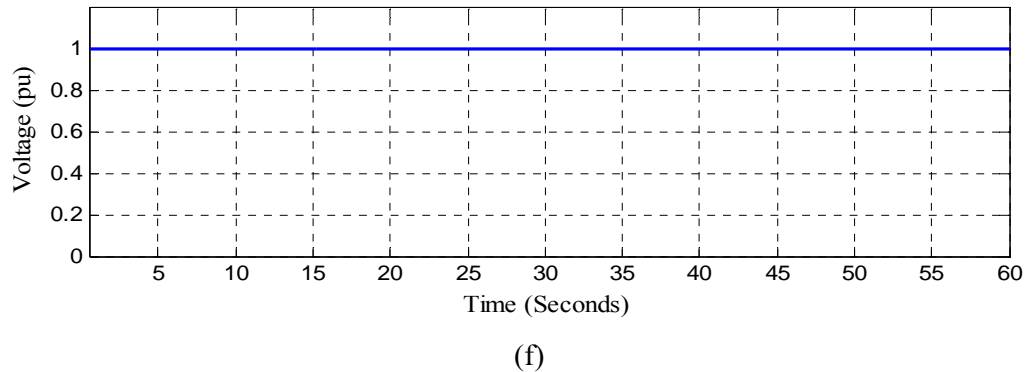
Fig. (4). (**a**). System frequency, (**b-c**) WPGS real and reactive power (**d-e**) HGU real and reactive power, (**f**) Voltage at bus-1.

However, in Mode-III, the wind speed is assumed to be zero after t = 5 seconds to reflect insufficient wind condition. The number of wind turbines in operation in the WPGS during an isolated mode depends on the micro-grid load demand and the wind availability, and is determined by the control coordinator. The grid is isolated from the system at t = 5 seconds because of a fault (unintentional islanding) or regular maintenance (intentional islanding) in the transmission systems. The interruption is simulated using a three phase circuit breaker with specific time settings.

MODE-I: GRID CONNECTED SYSTEM

The simulation results for Mode-I are represented in Fig. (**4a-f**). The system frequency is at its rated value and is shown in Fig. (**4a**). Figs. (**4b**) and (**4c**) show the real power generated and reactive power consumed by the WPGS while nine wind turbines are in operation. The output of the WPGS varies due to the wind speed variation. The real and reactive powers generated by the HGU are shown in Figs. (**4d**) and (**4e**). Voltage at bus 1 is shown in Fig. (**4f**). The voltage at bus 1 of the system is at its rated value. These results indicate that the operation of the HGU and WPGS in grid connected mode is dictated by the grid with the rated system voltages and frequency set by the grid. This also indicates that there is no power imbalance between loads and generation. It is worth mentioning that although the results in Mode-I are obvious, the results are presented as a reference for demonstrating the comparisons of micro-grid behaviours during various operational modes.

MODE-II: ISOLATED SYSTEM WITH WIND POWER GENERATION

The micro-grid system operates in Mode-I until t = 5 seconds. At t = 5 seconds, the grid is isolated from the system. Fig. (**5a**) shows the micro-grid frequency variation during transition from the grid connected to the isolated mode and in subsequent operation, which indicates an imbalance between power generation and consumption. It is to be noted that the frequency deviation is such that the generator will trip because of the system protection. However, this deviation is presented to show extreme conditions and to check the exact frequency deviation during the transition from Mode-I to Mode-II. Figs. (**5b**) and (**5c**) show the real power contribution and reactive power consumption by the WPGS during this mode when only one wind turbine is in operation in the WPGS. The real and reactive power generations by the

HGU are shown in Figs. (**5d**) and (**5e**). The real and reactive power consumed by the Loads is shown in Figs. (**5f-i**). The load power is reduced by a small amount after grid isolation because of the reduction in the system voltages caused by the lack of sufficient reactive power in the isolated micro-grid system. The lack of sufficient reactive power in the micro-grid system results in reduced voltage levels at the micro-grid system buses (Figs. **5j-k**). More than one wind turbine operating in the WPGS will deliver more active power in the micro-grid system than the load demand. The reactive power demand will also increase in the micro-grid system which will result in further reduction in voltage level at different buses in the micro-grid system.

MODE-III: ISOLATED SYSTEM WITHOUT WIND POWER GENERATION

The system operation follows the Mode-I until t = 5 seconds. However, at t = 5 seconds, the grid is isolated from the system. Concurrently, the WPGS has no output power as there is insufficient wind resource to produce electricity. The results of this mode of operation are shown in Figs. (**6a-h**). Fig. (**6a**) shows the micro-grid frequency fluctuation which is not as widely variable as in Mode-II; however, the variation is still not in the tolerable range (59.5-60.3) for micro-grid operation. The frequency fluctuation is not as wide as in Mode-II because of the wind turbines' disconnection due to insufficient wind speed from the system. The real and reactive powers generated by the HGU are shown in Figs. (**6d**) and (**6e**), respectively. The HGU generates rated value real power because this is the only real power generation unit in the micro-grid. As well, the reactive power demand is lower than the Mode-II. The load power shown in Figs. (**6f-g**) is lower than that in Mode-II, as the power generated by the micro-grid system is lower than the load demand. This implies the requirement of additional power from a reliable generation unit. The voltage level at bus 1 is shown in Fig. (**6h**), which is lower than the rated voltage. This fact indicates that there is a need for reactive power adjustment in the micro-grid system.

The simulation test results presented and discussed in above sections explore the problems related to the operation and control of the proposed wind-hydro power generation based micro-grid system and can be summarized as:

- Active power imbalance between generation units and loads in isolated micro-grid mode when wind power is available.

(a)

(b)

(c)

(d)

(e)

(f)

(g)

(h)

(i)

(j)

(k)
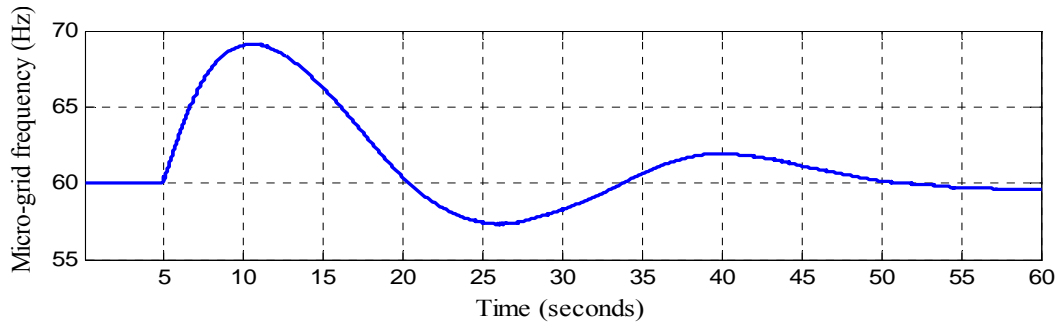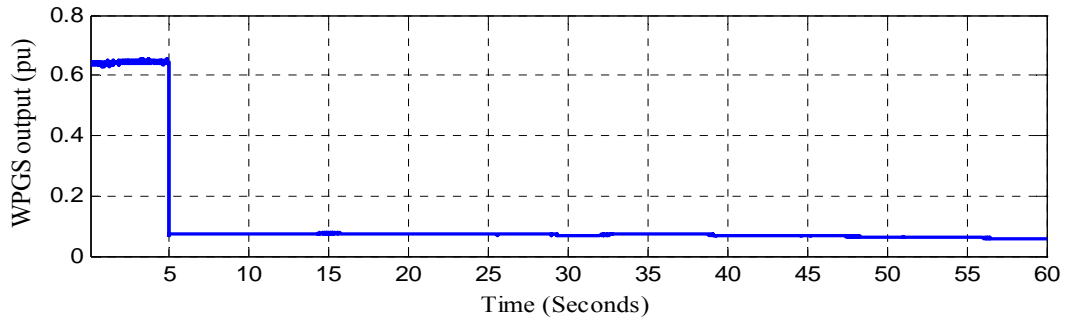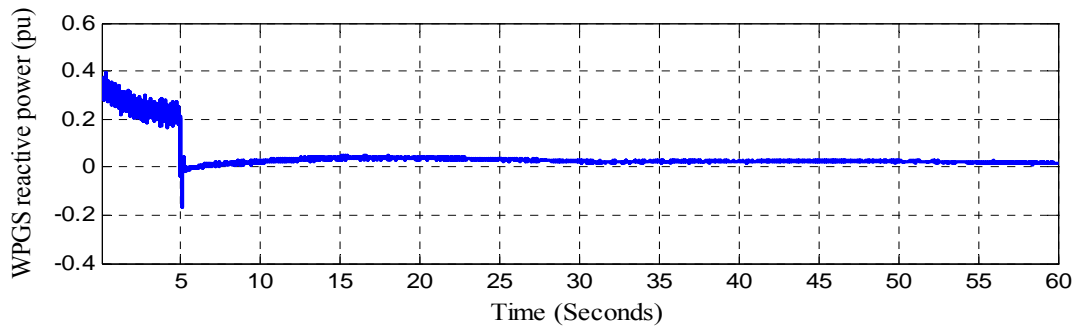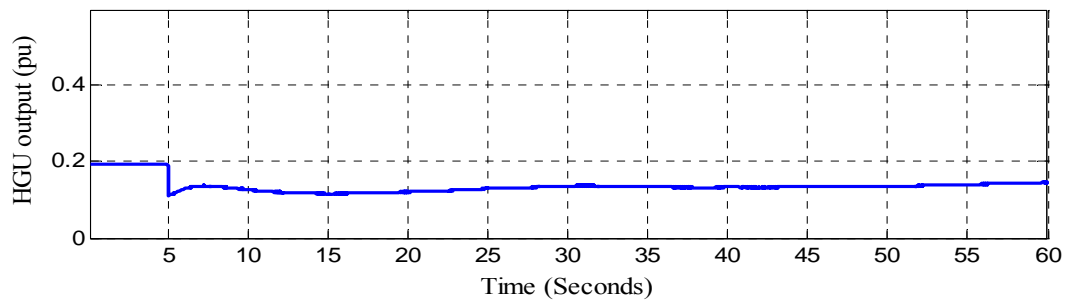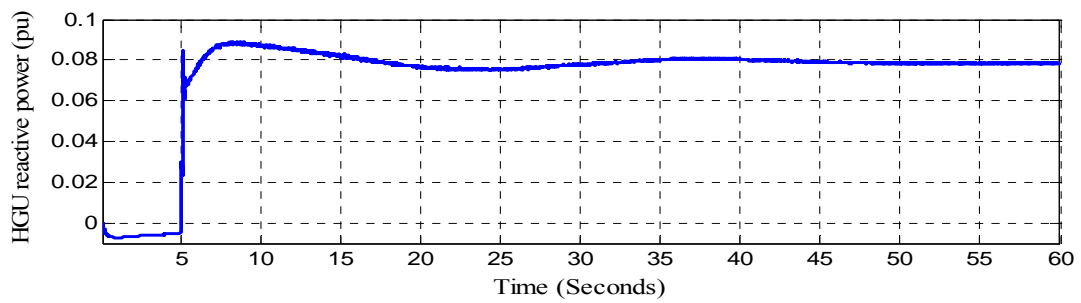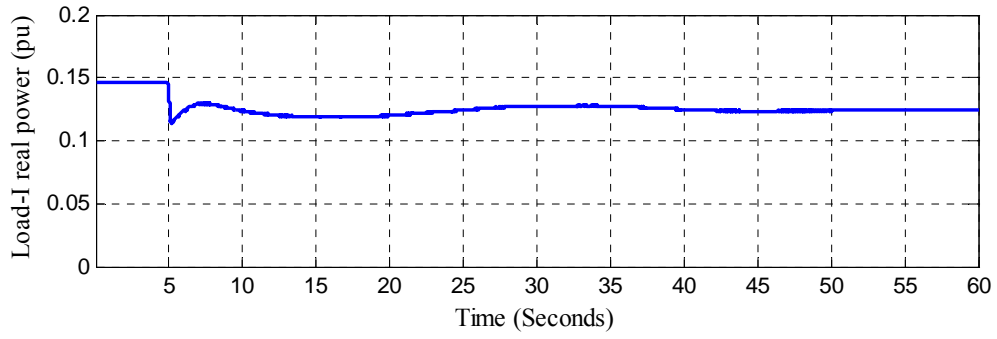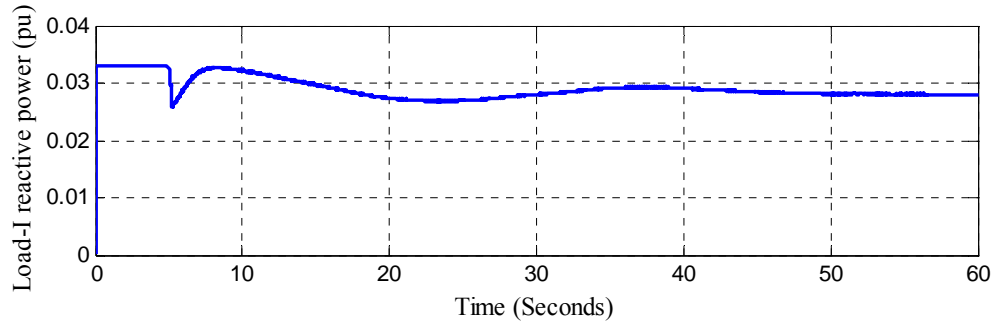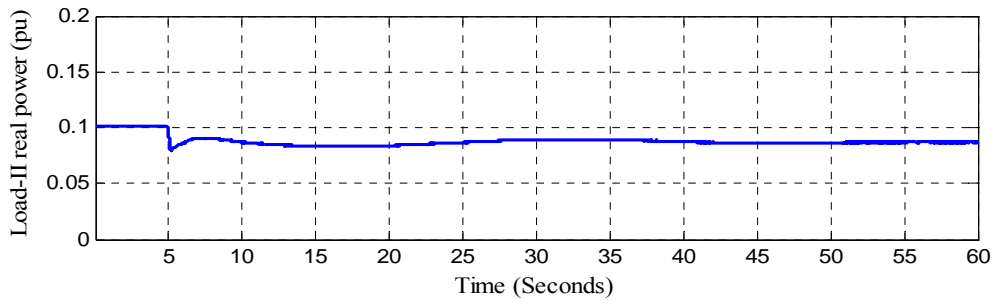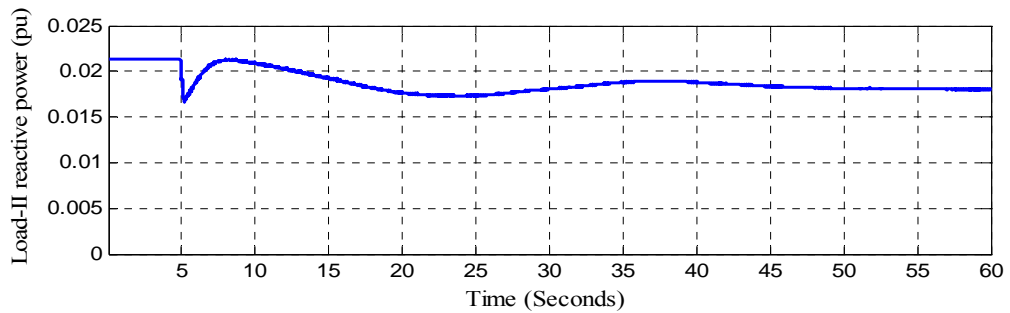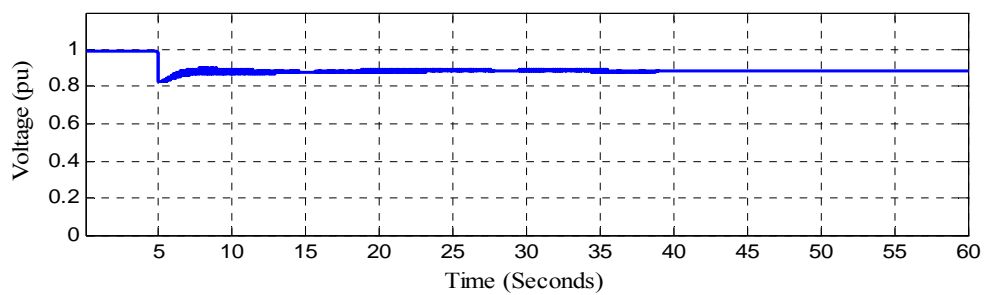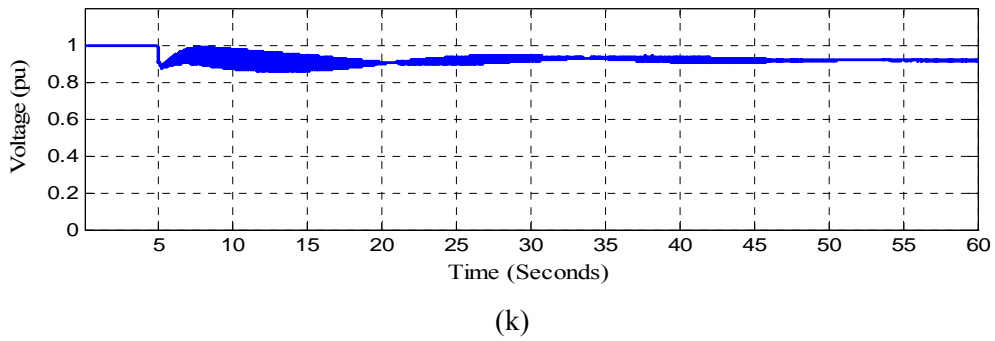
Fig. (5). (**a**). Micro-grid frequency, (**b-c**) WPGS real and reactive power, (**d-e**) HGU real and reactive power, (**f-i**) Load-I and Load-II real and reactive power demand, (**j-k**) Voltage at bus-1 and Load bus-I.

(a)

(b)

(c)

(d)
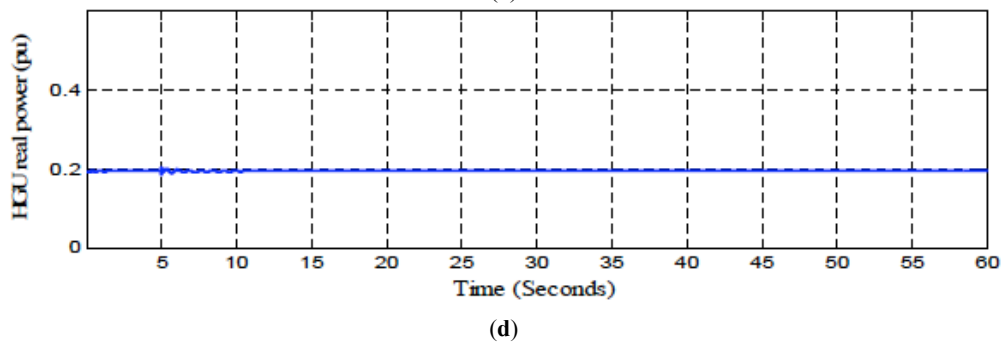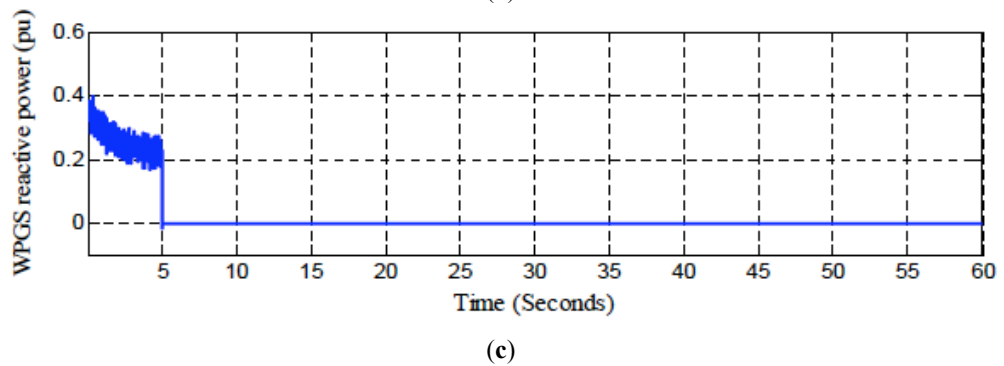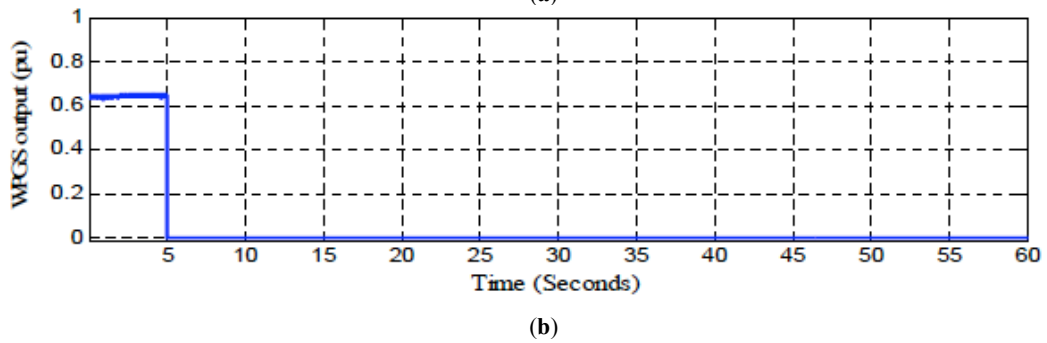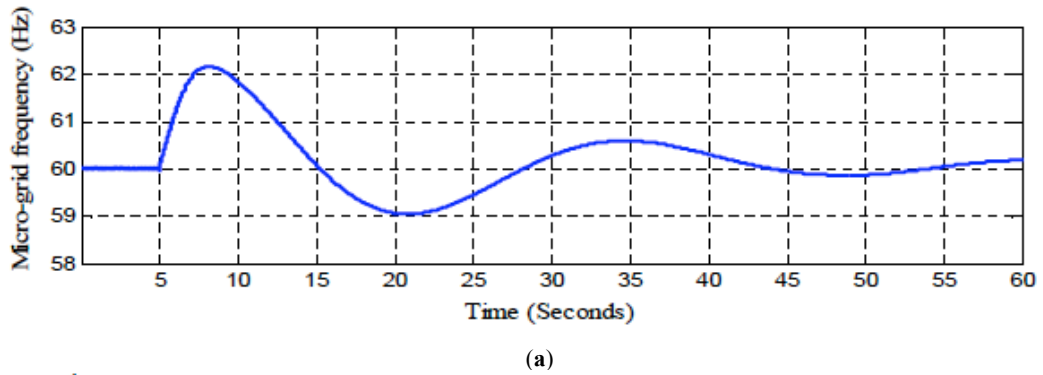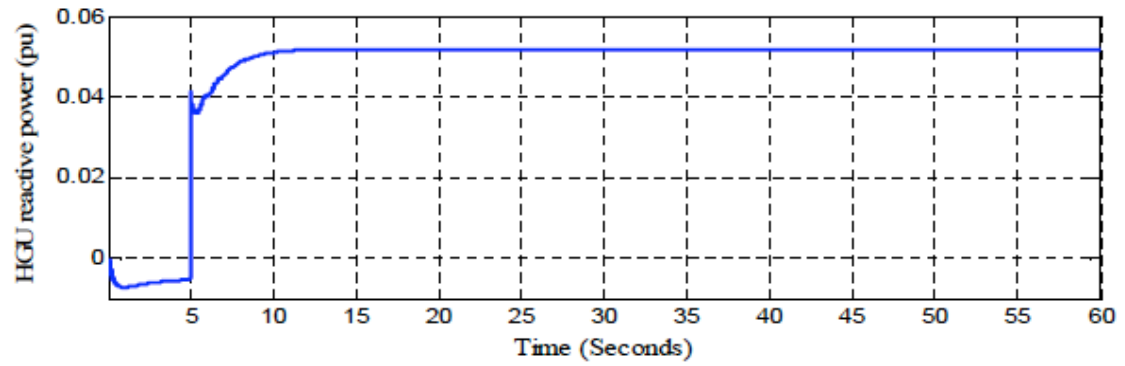
(e)
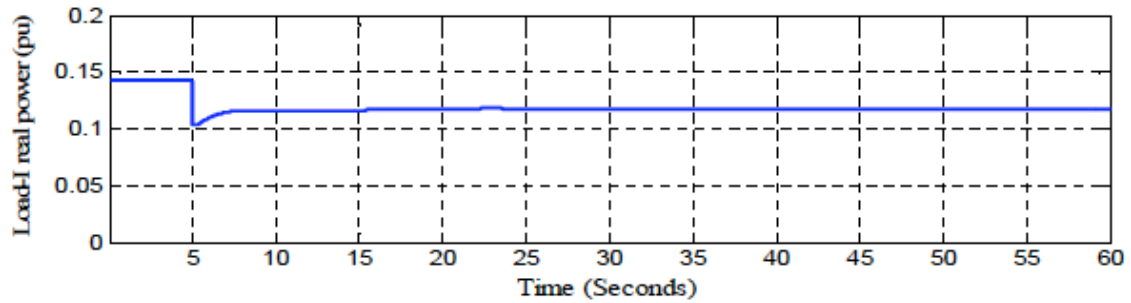
(f)
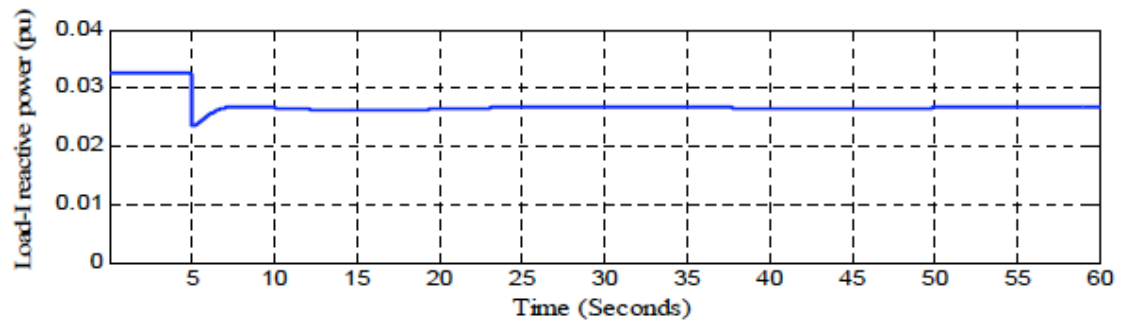
(g)
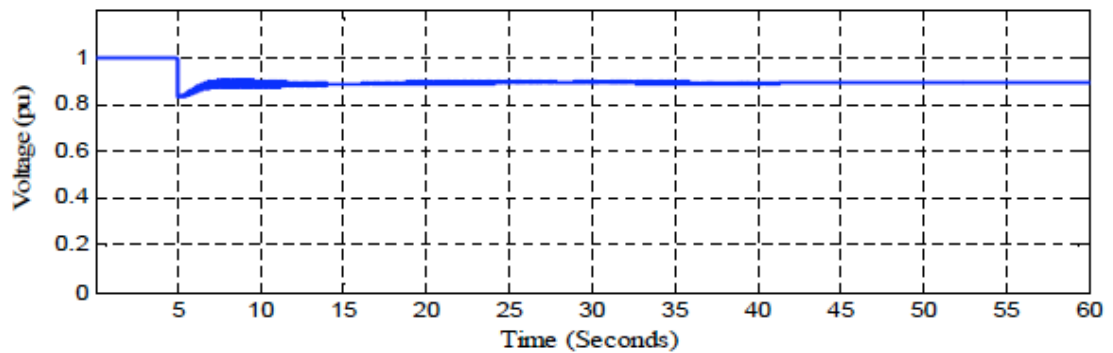
(h)

Fig. (6). (a). Micro-grid frequency, **(b-c)** WPGS real and reactive power, **(d-e)** HGU real and reactive power, **(f-g)** Load-I real and reactive power demand, **(h)** Voltage at bus 1.

- Active power imbalance between generation units and loads when wind power is not available in isolated micro-grid mode.

- Reactive power is required during isolated micro-grid operation to maintain the expected voltage level at different buses in the micro-grid system.

- Need for reliable energy storage in isolated micro-grid mode.

A dump load will also be needed to maintain the active power balance between generation and loads in isolated micro-grid mode when wind power is available. The reactive power demand can be provided by STATCOM during the
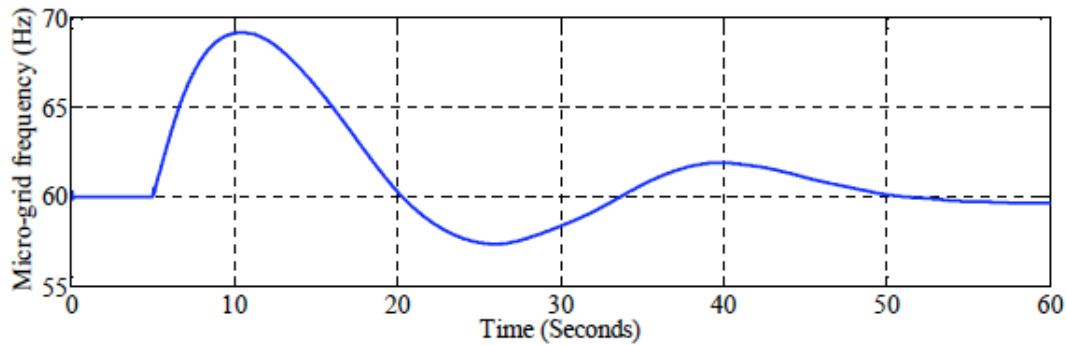
Fig. (7). Micro-grid frequency while the generator parameters are increased by 50 percent during the isolated micro-grid with wind power generation.
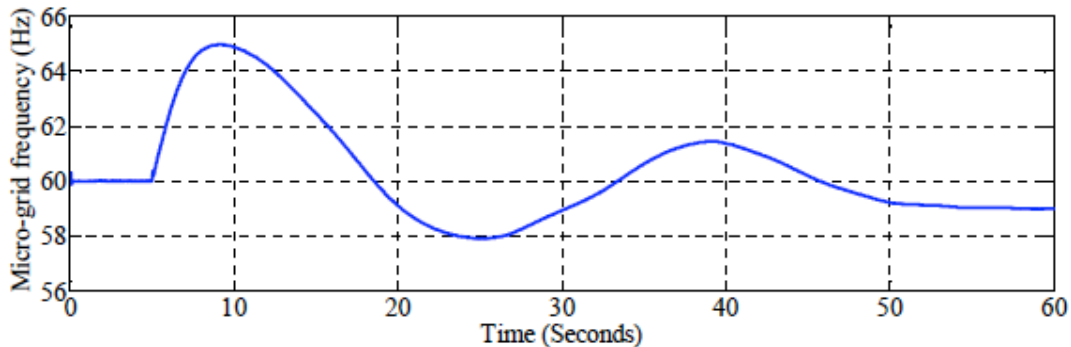
Fig. (8). Micro-grid frequency while the generators rated power is reduced by 25 percent during the isolated micro-grid with wind power generation.

operation of the isolated system with wind power and by the storage unit during the operation of the isolated system without wind power.

MODEL VALIDATION

The validation of system dynamic models can be carried out in numerous ways such as the field test, theoretical test, parameter sensitivity test and extreme-condition test [20]. A parameter sensitivity test is found for the generator model validation in [21]. Thus, the developed dynamic model of the study's micro-grid system is validated with a system parameter sensitivity test. The validation is performed by simulating the developed model with a change in induction and synchronous generator parameters. Such changes includes an increase in stator and rotor resistances, leakage inductances, mutual inductances, friction coefficient, and a reduction in generators' rated power. The simulation results are presented for the operating mode of an isolated micro-grid with wind power generation and an isolated micro-grid without wind power generation.

MODE-II: ISOLATED SYSTEM WITH WIND POWER GENERATION

Case A: Generator Parameters Variation

The developed model is simulated during the operating mode of an isolated micro-grid with wind power generation where the generator parameters are increased by 50 percent. The parameters for both induction and synchronous generators include stator and rotor winding resistances, leakage inductances, mutual inductances and friction coefficients. The micro-grid system frequency response is shown in

Fig. (**7**) under the condition of generator parameters variation. Although the variation in parameters is significant, the system frequency response is consistent with the response that is shown (Fig. **5a**) without the change in the generator parameters. This frequency response indicates the developed model insensitivity with the change in generators parameters.

Case B: Variation in Generators Rated Power

A simulation is carried out using the developed model of the micro-grid system during the operating mode of an isolated micro-grid with wind power generation where the generator powers are decreased by 25% percent. Such a variation also requires a necessary change in wind turbine and hydro turbine parameters. Considering those variations, the simulated micro-grid system frequency response is shown in Fig. (**8**). The behaviour of the system frequency during this condition is also similar to the one that is shown without the change in the generator rated powers. However, the initial deviation in the system frequency is lower than that of the frequency response shown in Fig. (**5a**) without the reduction in generators rated power. This result reveals that the dynamic behaviour of the micro-grid system frequency represents a similar pattern as is shown in Fig. (**5a**) with the disturbance in generators rated power.

MODE-III: ISOLATED SYSTEM WITHOUT WIND POWER GENERATION

Case A: Generator Parameters Variation

The performance of the developed model is investigated during the operating mode of an isolated micro-grid without wind power generation under the generator parameters varia-
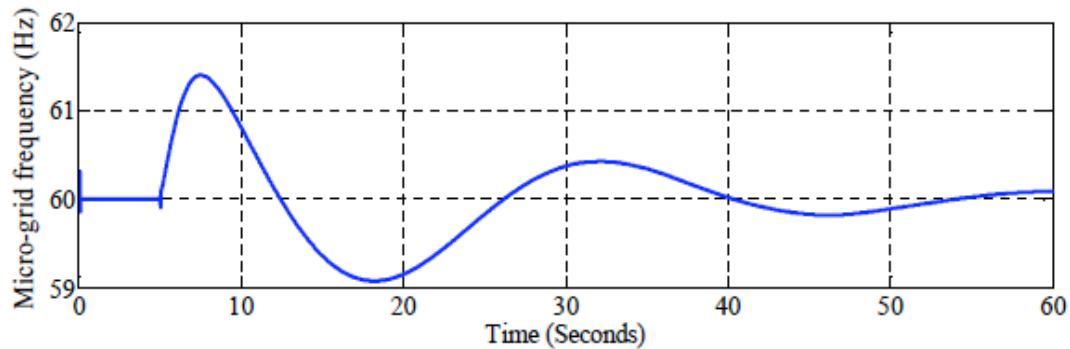
Fig. (9). Micro-grid system frequency during the operating mode of an isolated micro-grid without wind power generation while the generator parameters are increased by 50 percent.
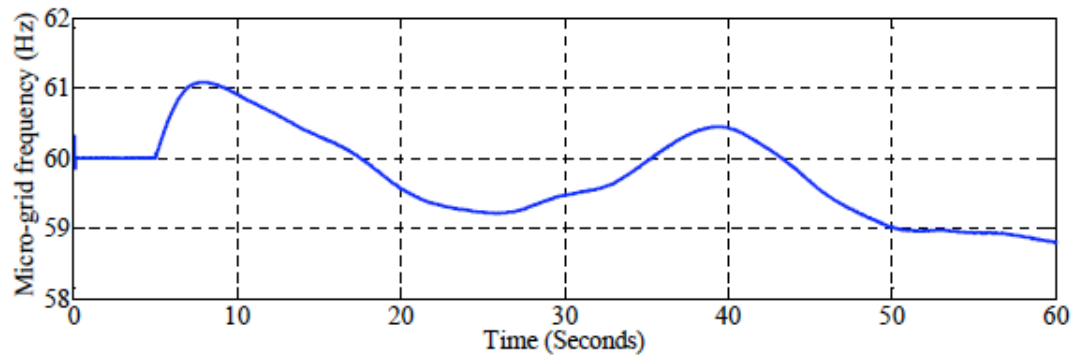
Fig. (10). Micro-grid frequency while the generator rated power is reduced by 25 percent during the operating mode of an isolated micro-grid without wind power generation.

tion. The parameters such as the stator and rotor winding resistances, leakage inductances, mutual inductances and friction coefficients of the synchronous generator are increased by 50% for this case study. Fig. (**9**) shows the micro-grid system frequency response considering the variation of the generator parameters. The system frequency deviation followed by the utility grid disconnection and in subsequent operation shows a similar pattern to the frequency response shown in Fig. (**6a**). Such a dynamic behaviour implies the insensitivity of the developed micro-grid model with the variation in generator parameters.

Case B: Reduction in Generator Rated Power

A simulation is carried out to observe the performance of the system frequency during the operating mode of an isolated micro-grid without wind power generation while taking into account a reduction in generator rated power of 25% percent. The performance of the micro-grid system frequency during this operating mode is shown in Fig. (**10**). The dynamic behaviour of the micro-grid system frequency shows consistent variation with the frequency response shown in Fig. (**6a**). Moreover, the initial deviation in the system frequency is also lower than that of the frequency response shown in Fig. (**6a**). However, the tendency of the system frequency is going to be below the system rated frequency as time passes. This is because the HGU is the only electricity generation unit in the micro-grid during this operating mode (Mode-III). Also the rated power of the HGU unit is further reduced by 25 percent. Thus the insufficient power generation in the micro-grid results in the system frequency pattern as shown in Fig. (**10**).

ADDITIONAL REQUIREMENTS AND PROPOSED CONTROL CONCEPTS FOR MICRO-GRID OPERATION

The system frequency and the required voltage level for the load are decided by the utility grid during the utility grid-connected operation. Any abnormal condition occurring in the upstream power line which is not cleared within the fault clearing time set by the utility grid will result in system isolation. In order to operate the proposed micro-grid system during the isolated mode, the system requires rearranging with additional components such as storage system, STAT-COM, dumping load as well as controlling strategies. The isolated microgrid system with additional components can be represented conceptually as in Fig. (**11**). Moreover, a voltage and frequency controller, control coordinator and monitoring system would be required to ensure reliable operation of the micro-grid system. During the isolated mode, the number of wind turbines in operation depends on the load demand and wind availability, which is determined by the control coordinator. Functions of the control co-ordinator and monitoring system can be performed based on the state diagram shown in Fig. (**12**).

In order to ensure reliable operation of the micro-grid system over the entire range of operational conditions, a control concept is proposed and briefly outlined. Fig. (**13**) shows the block diagram representation of the proposed control concepts for reliable and stable operation of the proposed wind-hydro power generation based microgrid system.

- Control coordinator and system monitoring: The main functions of this subsystem are to: (i) detect the sys-
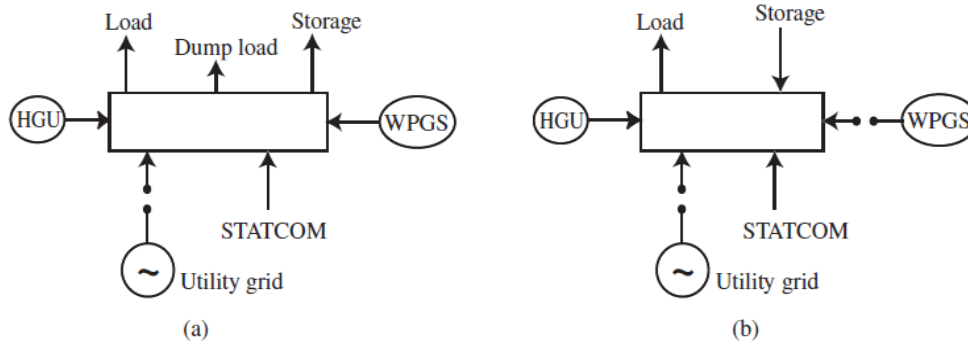
Fig. (11). Functional block diagram of the micro-grid operating modes: (**a**) Isolated micro-grid system with wind generator, (**b**) Isolated micro-grid system without wind generator.
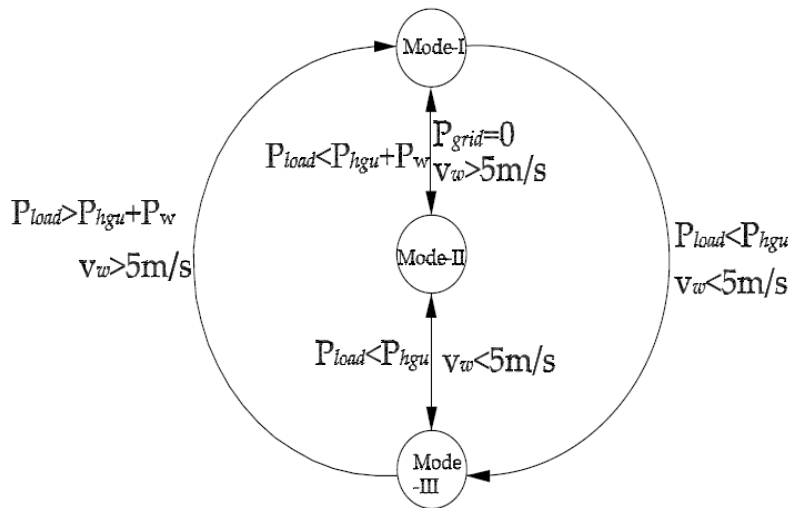
Fig. (12). State diagram for operational modes of the micro-grid system.
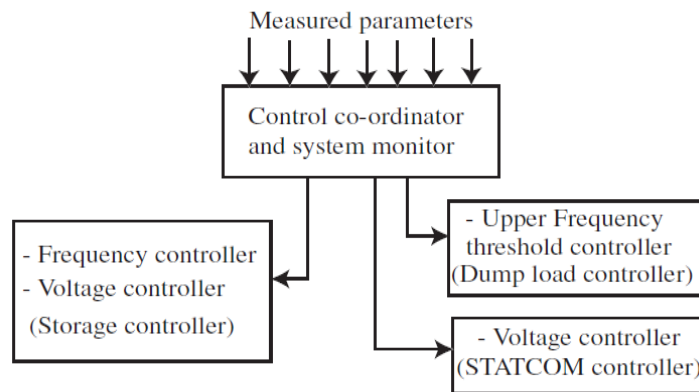
Fig. (13). Proposed control and micro-grid system management concepts.

tem islanding, (ii) activate the operating modes of the microgrid system with the proper frequency and voltage controller, (iii) manage the wind turbine operation in the WPGS, (iv) monitor grid recovery and, (v) synchronize the grid. A load flow based micro-grid monitoring and control coordinator scheme is chosen to determine the power status at the buses of the proposed micro-grid system. The load flow problem for a micro-grid system with few buses can be solved with fewer computational complexities.

- Upper frequency threshold controller (Dump load controller): The objective of this control subsystem is to maintain the micro-grid frequency between 59.5-60.3Hz, while the HGU and WPGS deliver power to the microgrid. The controller will maintain frequency by balancing the active power between the generation and load, either by dumping power into the dump load or releasing power from it, and/or by storing energy using motor-pump units for pumping water into the upper reservoir.

- Lower frequency threshold controller (Storage system controller): The objective of this control subsystem is to maintain the micro-grid frequency between 59.5-, 60.3Hz, while the micro-grid generated power is less than the load demand because of the lack of wind speed. The controller will maintain frequency by balancing the active power between the generation and load using the pumped hydro storage system or another fast response power electronic interface storage system.

- Voltage controller: The objective of this control subsystem is to maintain the micro-grid voltage at a desired level. The controller will maintain voltage level by balancing the reactive power in the micro-grid system. The control subsystem will ensure that during isolated mode with wind power generation the STATCOM will provide reactive power balance in the system. Similarly, during isolated mode without wind power generation the storage unit or STATCOM will provide reactive power balance in the micro-grid system.

CONCLUSIONS

This paper presents a micro-grid system powered by renewable energy sources such as wind and hydro. Three operational modes dictated by the availability of the grid and the wind power generation unit are identified for operation of the proposed micro-grid system. The models of the components of the proposed system are developed and used in a MATLAB/SIMULINK simulation in order to study the operational behaviours of the micro-grid system. The micro-grid system behaviour is also observed with a change in generator parameters and in the generators' rated power, which indicates the sensitivity of the developed model. The system behaviours in each mode reveal the technical challenges and the additional necessities for operating the proposed wind-hydro source based micro-grid system. Such issues as well as the conceptual approaches for addressing some of the issues are presented in this paper. The control and management protocol outlined in this paper is required to be developed along with additional components for stable and autonomous operation of the proposed micro-grid system.

CONFLICT OF INTEREST

The authors confirm that this article content has no conflicts of interest.

ACKNOWLEDGEMENTS

ABBREVIATIONS

CERTS	=	Consortium for electric reliability technology solutions
FC	=	Fuel cell
HGU	=	Hydro generation unit
MG	=	Micro-grid
MCFC	=	Molten carbonate fuel cell
NEDO	=	New energy and industrial technology development organization
PV	=	Photovoltaic
PCC	=	Point of common coupling
PAFC	=	Phosphoric acid fuel cell
SOFC	=	Solid oxide fuel cell
WT	=	Wind turbine
WPGS	=	Wind power generation system

LIST OF SYMBOLS

A_{SA}	=	Swept area covered by the turbine rotor
C_p, C_P	=	Power coefficient
V_W	=	Wind velocity
R_t	=	Radius of turbine rotor
β	=	Pitch angle of rotor blades
λ_i	=	Intermediate variable to calculate tip speed ratio
ρ	=	Air density
ω_m	=	Angular velocity of turbine rotor
r_s, r_r'	=	Stator and rotor winding resistance
$L_{ls}\, L_{lr}'$	=	Leakage inductance of stator and stator winding
L_m	=	Magnetizing inductance
V_{ds}, V_{qs}	=	d and q components of stator voltage
V_{dr}', V_{qr}'	=	d and q components of rotor voltage
i_{ds}, i_{qs}	=	d and q components of stator current
i_{dr}', i_{qr}'	=	d and q components of rotor current
$\varphi_{ds}, \varphi_{qs}$	=	d and q components of stator flux linkage
ϕ_{dr}', ϕ_{qr}'	=	d and q components of rotor flux linkage
ω_e	=	Speed of the synchronously rotating reference frame
ω_r	=	Electrical angular speed of the rotor
ω_{rm_IM}	=	Mechanical angular speed of the induction motor rotor
T_{m_WT}	=	Wind turbine torque
J_{WG}	=	Moment of inertia for wind generator
F_{WG}	=	Friction co-efficient for wind generator
r_{ss}	=	Synchronous machine stator winding resistance
r_{fd}'	=	d-axis field winding resistance
$r_{kd}', r_{kq1}', r_{kq2}'$	=	d and q-axis damper winding resistances
L_{lss}	=	Leakage inductance of the synchronous machine stator winding
L_{lfd}'	=	Leakage inductance of the d-axis field winding

L'_{lkd} , L'_{lkq1} , L'_{lkq2}	=	Leakage inductances of the d and q-axis damper windings
L_{md}, L_{mq}	=	d and q-axis magnetizing inductance
L_d, L_q	=	d and q-axis combined inductance of leakage and magnetizing component
V_d, V_q	=	d and q axis stator voltage component of synchronous machine
V'_{fd}	=	d-axis field voltage component
V'_{kd} , V'_{kq1} , V'_{kq2}	=	d and q-axis damper winding voltages
i_d, i_q	=	d and q axis current component of synchronous motor stator
i'_{fd}	=	d-axis field current
i'_{kd} , i'_{kq1} , i'_{kq2}	=	d and q-axis damper winding currents
φ_d, φ_q	=	Stator d and q-axis flux linkage component
ϕ'_{fd}	=	d-axis field winding flux linkage
ϕ'_{kd} , ϕ'_{kq1} , ϕ'_{kq2}	=	d and q-axis damper winding flux linkage
ω_{rm_SM}	=	Mechanical angular speed of the synchronous machine rotor
T_m	=	Mechanical torque
J_{SM}	=	Inertia co-efficient of synchronous machine
F_{SM}	=	Friction co-efficient of synchronous machine
q	=	Turbine flow rate
H_0	=	Water column static head
H	=	Head at the turbine inlet
H_L	=	Head loss due to friction
g	=	Acceleration
A_{pen}	=	Cross sectional area of the penstock
L	=	Length of the penstock
$\bar{H}$	=	Per unit head at the turbine inlet
$\bar{P}_m$	=	Mechanical power in per unit
$\bar{q}_{nl}$, $\bar{q}_{fl}$	=	Per unit water flow at no load and full load
A_{TG}	=	Turbine gain $= \dfrac{1}{(g_2 - g_1)}$
g_1, g_2	=	Gate opening at full load and no load
G	=	Gate position

REFERENCES

[1]   Blaabjerg, F.; Teodorescu, R.; Liserre, M.; Timbus, A.V. Overview of control and grid synchronization for distributed power generation systems. *IEEE. Trans. Indust. Electron.,* **2006**, *53*, 1398-1409.

[2]   Katiraei, F.; Abbey, C.; Bahry, R. Analysis of voltage regulation problem for 25kv distribution network with distributed generation. In: *IEEE Power Engineering Society General Meeting*, Montreal, Canada, June, **2006**.

[3]   Lasseter, R.H. *Micro-grids*. In: IEEE Power engineering society winter meeting, New York, US, January, **2002**.

[4]   Barnes, M.; Dimeas, A.; Engler, A.; Fitzer, C.; Hatziargyriou, N.; Jones, C.; Papathanassiou, S. *Micro-grid Laboratory Facilities*. In: IEEE International conference on future power system, The Netherlands, November, **2005**. Also find www.microgrids.eu.

[5]   MICROGRIDS-large scale integration of micro-generation to low voltage grids. EU Contract ENK5-CT-2002-00610, Technical Annex, May **2002**. Also find http://microgrids.power.ece.ntua.gr.

[6]   Hatziargyriou, N.; Asano, H.; Iravani, M. R.; Marnay, C. Microgrids- An overview of ongoing research, development and demonstration projects. *IEEE Power Energy Mag*, **2007**, 78-94.

[7]   Morozumi, S. *Overview of micro-grid research and development activities in Japan*. In: A Symposium on Micro-grids, Montreal, Canada, June, **2006**.

[8]   Abbey, C.; Katiraei, F.; Brothers, C. *Integration of distributed generation and wind energy in Canada*. In: IEEE Power Engineering Society General Meeting, Montreal, Canada, June, **2006**.

[9]   Katiraei, F.; Iravani, M. R.; Lehn, P.W. Small signal dynamic model of a micro-grid including conventional and electronically interfaced distributed resources. *IET. Gener. Transm. Dis.,* **2007**, *1*, 369-378.

[10]   Shahabi, M.; Haghifam, M. R.; Mohamadian, M.; Nabavi-Niaki, S. A. Micro-grid dynamic performance improvement using a doubly fed induction wind generator. *IEEE. Trans. Energy Convers,* **2009**, *24*, 137-145.

[11]   Majumder, R.; Ghosh, A.; Ledwich, G.; Zare, F. Load Sharing and Power Quality Enhanced Operation of a Distributed Micro-grid. IET Renew. *Power. Gener.,* **2009**, *3*, 109-119.

[12]   Nayar, C. *Remote Area Micro-Grid System using Diesel Driven Doubly Fed Induction Generators*, Photovoltaics and Wind Generators. In: IEEE International Conferences on Sustainable Energy Technologies, Singapore, November, **2008**.

[13]   Slootweg, J. G.; De Haan, S. W. H.; Polinder, H.; Kling, L. W. General Model for Representing Variable speed wind turbines in power system dynamics simulations. *IEEE. Trans. Power. Sys.,* **2003**, *18*, 144-151.

[14]   Heier, S. *Grid integration of wind energy conversion system*. 2nd ed., Wiley-Chicester, U.K, **2006**.

[15]   Krause, P. C.; Wasynczuk, O.; Sudhoff, S. D. *Analysis of electric machinery and drive systems*. 2nd ed., IEEE Press, **2002**.

[16]   IEEE working group on prime mover and energy supply models for system dynamic performance studies. Hydraulic Turbine and Turbine Control Models for Dynamic Studies. *IEEE. Trans. Power. Sys.,* **1992**, *7*, 167-179.

[17]   Katiraei, F.; Iravani, M. R.; Lehn, P. W. Micro-grid autonomous operation during and subsequent to islanding process. *IEEE. Trans. Power. Deliv.*, **2005**, *20*, 248-259.

[18]   Mechanical operating and maintenance. Manual V90 - 3.0 MW, VCRS 60 Hz-Class II, Item no.: 964106.R00, **2007**.

[19]   Gaillard, A.; Poure, P.; Saadate, S.; Machmoum, M. Variable speed dfig wind energy system for power generation and harmonic current mitigation. *RenE, J.,* **2009**, *34*, 1545-1553.

[20]   Barlas, Y. Formal aspects of model validity and validation in system dynamics. *Sys. Dyn. Rev.,* **1996**, *12*, 183-210.

[21]   Khan, M. A. *A wavelet packet transform based on-line technique for protection of three phase interior permanent magnet synchronous motors*. Master's Thesis, Memorial University of Newfoundland, **2006**.